

The normal state scattering rate in high- T_c cuprates

N.E. Hussey

H. H. Wills Physics Laboratory, University of Bristol, Bristol, BS8 1TL, United Kingdom.

(December 2, 2024)

I present a new phenomenological model for the normal state transport properties of high- T_c cuprates. In particular, I identify a form of scattering rate that may account, both qualitatively and quantitatively, for all the low-field normal state (magneto)-transport properties of the single-band single-layer cuprate $\text{Ti}_2\text{Ba}_2\text{CuO}_{6+\delta}$ from optimal doping through to the overdoped side of the phase diagram. The form of the scattering rate is also consistent with features seen in photoemission spectroscopy in high- T_c cuprates and offers a new intuitive way to understand the variation of T_c with carrier concentration.

PACS numbers: 72.10.-d, 74.25.Fy, 74.72.Fq

I. INTRODUCTION

The search for a consistent description for the anomalous normal state transport properties of high- T_c cuprates (HTC) has been a long and fascinating journey. Many phenomenological models seeking to identify the appropriate form for the normal state scattering rate have been offered but none have captured the complete picture. From the very beginning, it was clear that the T -linear behavior of the in-plane resistivity ρ_{ab} , extending over an anomalously broad range of temperature for optimally doped (OP) cuprates, would be difficult to reconcile within a conventional Fermi-liquid (FL) framework.¹ Later observations of the T^2 dependence and impurity dependence of the inverse Hall angle $\cot\Theta_H$,² together with the modified Kohler's rule (in-plane orbital magnetoresistance $\Delta\rho_{ab}/\rho_{ab} \sim \tan^2\Theta_H$),³ seemed to constitute an insurmountable challenge to FL theory and new approaches were sought.

Several notable attempts to explain this anomalous behavior within a modified FL scenario followed, each one incorporating a particular form for the (strong) anisotropy of the transport scattering rate within the plane arising out of some form of coupling to a singular bosonic mode; be it spin fluctuations,^{4,5} charge fluctuations⁶ or d -wave superconducting fluctuations.⁷ In each case, however, inconsistencies with certain aspects of the experimental data were exposed.

Given these failings, other more exotic models, based on a non-FL ground state, gained prominence within the community; most notably the two-lifetime picture of Anderson⁸ and the Marginal-Fermi-liquid (MFL) model of Varma and co-workers.⁹ In contrast to the FL scenarios, the scattering rates that govern the T -dependence of the normal state transport properties in both these models are assumed to be momentum independent (though Varma *et al.* have recently introduced anisotropy into their model, via forward scattering on impurities, to account for the observed magnetotransport behavior¹⁰). In the two-lifetime approach, scattering processes involving momentum transfer parallel and perpendicular to the Fermi surface are governed by independent scattering rates with different T -dependencies. This model has

been extremely insightful for understanding the transport phenomena in OP cuprates, but has yet to provide a consistent explanation for the results of Angle-Resolved Photoemission Spectroscopy (ARPES) or the evolution of the transport behavior across the HTC phase diagram. The MFL hypothesis assumes that optimum T_c lies in proximity to a quantum critical point and consequently, quasi-particles are ill-defined everywhere on the Fermi surface with a self-energy that is governed simply by the temperature (or frequency) scale. In contrast to the two-lifetime picture, this model is consistent with certain aspects of ARPES measurements,¹¹ though not all. Most notably, the recently reported evidence of a kink in the energy dispersion¹² seems at odds with a scenario based on quantum criticality. Yet again, predictions of the MFL theory have so far been confined to optimum doping.

In this paper, I propose a new phenomenology for the normal state transport properties in HTC that has as its basis, two novel but physically reasonable assumptions. Firstly, the scattering rate is assumed to vary as T^2 everywhere on the Fermi surface, but in contrast to previous approaches, both the impurity *and* the T -dependent terms in the self-energy contain strong (doping dependent) basal plane anisotropy. The second key assumption is that this anisotropic scattering rate eventually saturates (on different regions of the Fermi surface at different temperatures) at a value equivalent to the well-known Mott-Ioffe-Regel (MIR) criterion for coherent band transport. With very few adjustable parameters, the model can account for *all* the anomalous dc transport properties of OP HTC as described above, whilst at the same time retaining key elements of ARPES. Moreover, the model goes beyond previous proposals in that it can also account for the evolution of the observed normal state behavior across the overdoped (OD) region of the phase diagram from optimum doping. Taking $\text{Ti}_2\text{Ba}_2\text{CuO}_{6+\delta}$ ($\text{Ti}2201$) as our model HTC system, both qualitative and quantitative agreement is found between the model and experimental data for $\rho_{ab}(T)$, $\cot\Theta_H(T)$ and importantly, the magnitude and T -dependence of $\Delta\rho_{ab}/\rho_{ab}(T)$. In the process, we challenge two of the previously established paradigms of the normal state in HTC; namely the

linear low- T behavior of $\rho_{ab}(T)$ and the relevance of the non-saturating $\rho_{ab}(T)$ observed at higher temperatures.

In section II, I summarize the salient features of the model and in section III, I apply the Jones-Zener expansion to the linearized Boltzmann transport equation and compare the model with experimental data on Tl2201 at different doping concentrations. Finally, in section IV, I explain the physical justification for our particular choice of scattering rate and discuss the implications of this phenomenological model for the physics of HTC across the phase diagram, suggesting possible directions for further study.

II. THE MODEL

With its improved energy and momentum resolution, ARPES has now become a very powerful probe of the single-particle self-energy Σ of HTC. One of the most striking features of the emerging spectral function is the broad featureless normal state spectrum at the so-called "anti-nodal" points at $(\pi, 0)$ whose lineshape sharpens dramatically into the well-known peak-dip-hump structure upon cooling below T_c . Although interpretation of ARPES spectra remains controversial,¹³ it has been argued^{7,14} that this dramatic rearrangement of the ARPES lineshape indicates the presence of ill-defined quasi-particle states in the normal state at $(\pi, 0)$, rendered incoherent by some form of catastrophic low-energy scattering mechanism that is frozen out below T_c . This interpretation of ARPES provides a natural explanation for the sudden rise in the quasi-particle lifetime below T_c inferred from microwave conductivity¹⁵ and thermal conductivity¹⁶ measurements. ARPES data also reveal that the broadening of the quasi-particle self-energy above T_c is much less dramatic for the "nodal" quasi-particles at the (π, π) points and that this basal plane anisotropy is much larger for OP cuprates than for OD cuprates.¹⁷ All these features indicate highly anisotropic normal state scattering whose anisotropy grows weaker with overdoping.

The first direct evidence for in-plane anisotropy in the quasi-particle lifetime in HTC actually came from angular dependent studies of the c -axis magnetoresistance $\Delta\rho_c/\rho_c$ in OD Tl2201 ($T_c = 30\text{K}$).¹⁸ On rotating a magnetic field \mathbf{B} within the basal plane, $\Delta\rho_c/\rho_c$ was found to exhibit four-fold anisotropy with an amplitude that scaled as B^4 in accordance with Boltzmann transport analysis for an anisotropic quasi-two-dimensional (quasi-2D) Fermi surface. The ratio of the amplitude of these four-fold oscillations to the size of the higher order B^4 term in the isotropic (transverse) magnetoresistance showed a significant T -dependence from 30K to 150K (the temperature range of the experiment) that was interpreted as an increasing anisotropy of the in-plane scattering rate with increasing T . More importantly, the same analysis suggested that this T -dependent

anisotropy could explain, qualitatively at least, the T -dependence of the in-plane Hall coefficient R_H for this particular doping level.¹⁸

These observations, from both spectroscopic and transport measurements, constitute strong experimental evidence that the dominant scattering mechanism in HTC is highly anisotropic within the basal plane. In such a scenario, Ong has shown that the Hall angle $\tan\Theta_H(T)$ will be dominated by those regions of the Fermi surface where the scattering is weakest¹⁹, in this instance, the nodal points at (π, π) . By the same reasoning, I argue here that the T -dependence of $\cot\Theta_H(T)$ ($\sim A + BT^2$) is the *intrinsic* T -dependence of the scattering rate in HTC. A key assumption of the present model is that the scattering rate has the same quadratic T -dependence *everywhere* on the Fermi surface, but is highly anisotropic, being maximal along $(\pi, 0)$. Combined with an elastic scattering rate $\Gamma_0(\phi)$, which may also contain 4-fold anisotropy,¹⁰ the "ideal" scattering rate $\Gamma_{\text{ideal}}(\phi)$ may be written as

$$\Gamma_{\text{ideal}}(\phi) = \Gamma_0(\phi) + \Gamma_T(\phi)$$

where

$$\Gamma_0(\phi) = A(1 + c \cos^2(2\phi))$$

and the T -dependent scattering rate

$$\Gamma_T(\phi) = B(1 + e \cos^2(2\phi))T^2$$

Here ϕ represents the angle between the in-plane Fermi wave vector and the x -axis, whilst c and e are the anisotropy factors for the impurity and T -dependent scattering rates respectively. As mentioned above, $\Gamma_{\text{ideal}}(\phi)$ is largest along the anti-nodal direction $(\pi, 0)$ and smallest, but still finite, along (π, π) .

The second key feature of the model is the assumption that the MIR limit for coherent motion in a metal is also relevant for HTC. In its basic form, the MIR criterion states simply that the quasi-particle mean free path ℓ cannot become smaller than the lattice spacing a , since at this point, the quasi-particles lose their coherence and conventional Boltzmann transport analysis becomes irrelevant. When k -dependence is introduced, different regions of the Fermi surface begin to lose their coherence at different temperatures. Likewise, the scattering rate at different points on the Fermi surface will saturate (at the MIR limit) at different temperatures.

The first evidence for resistivity saturation in metals, consistent with the MIR limit, was reported in the A-15 compounds.²⁰ The T -dependence of the resistivity in this instance was found to fit extremely well to a simple "parallel resistor" model,²¹ suggesting that the ideal resistivity (i.e. the resistivity in the absence of saturation) was somehow shunted by a large saturation resistivity ρ_{max} corresponding to $\ell = a$. Using the MIR criterion as his guide, Gurvitch later argued²² that there must be a minimum time below which no scattering event can

take place, i.e. a minimum distance a over which each carrier gains additional drift velocity before being scattered, and from this derived an elegant understanding of the appropriateness of the parallel-resistor model for resistivity saturation.

In the spirit of Gurvitch's picture, I also introduce for HTC a maximum scattering rate (minimum scattering time) Γ_{\max} and define an effective scattering rate $\Gamma_{\text{eff}}(\phi)$ at each point on the Fermi surface of the parallel-resistor form

$$\frac{1}{\Gamma_{\text{eff}}(\phi)} = \frac{1}{\Gamma_{\text{ideal}}(\phi)} + \frac{1}{\Gamma_{\max}}$$

$\Gamma_{\text{eff}}(\phi)$ is then inserted into the Jones-Zener expansion of the standard Boltzmann transport equation (BTE) for a quasi-2D Fermi surface to extract all measurable transport coefficients. A derivation of the appropriate expressions is included in the Appendix. The value of Γ_{\max} for HTC can be estimated simply from $\ell = a$ since the Fermi velocity v_F in HTC is reasonably well known from band structure calculations and from ARPES measurements. Given $v_F = 1 - 3 \times 10^5 \text{ ms}^{-1}$, we estimate Γ_{\max} to be in the range 250 - 750 THz (150 - 450 meV).

The T -dependence of $\Gamma_{\text{eff}}(\phi, T)$ is illustrated schematically in Fig. 1 for the two most relevant momentum directions $(\pi, 0)$ and (π, π) . For concreteness, the parameters used in this simulation are the same as those used in the next section to fit the transport data for OP Tl2201, i.e. $A = 18 \text{ THz}$, $B = 9.3 \times 10^{-4} \text{ THz/K}^2$, $c = 8$, $e = 18$ and $\Gamma_{\max} = 500 \text{ THz}$. Along $(\pi, 0)$, $\Gamma_{\text{ideal}}(T)$ reaches Γ_{\max} at $T \sim 140\text{K}$, at which point the anti-nodal quasi-particles lose their coherence, in agreement with ARPES.²³ Due to the presence of the "shunt" Γ_{\max} , however, $\Gamma_{\text{eff}}(T)$ is always smaller than $\Gamma_{\text{ideal}}(T)$ and approaches saturation much more gradually. For the quasi-particles at (π, π) , $\Gamma_{\text{ideal}}(T)$ reaches Γ_{\max} at a much higher temperature ($T \sim 700\text{K}$). Hence, at the nodal points, well-defined coherent quasi-particles exist at all relevant temperatures. The "effective" anisotropy $e^* (= \Gamma_{\text{eff}}^{(\pi,0)}/\Gamma_{\text{eff}}^{(\pi,\pi)})$ is significantly lower than e for all finite T , reaching a maximum value $\sim e/2.5$ at the temperature where $\Gamma_{\text{ideal}}^{(\pi,0)}$ first crosses Γ_{\max} (see inset to Fig. 1). The overall effect is a transport scattering rate $\Gamma_{\text{eff}}(\phi, T)$ whose anisotropy initially grows with increasing T but then gradually becomes more isotropic at higher temperatures as the scattering rate at different regions of the Fermi surface tends towards saturation.

III. RESULTS

Having introduced the phenomenology for $\Gamma_{\text{eff}}(\phi, T)$, I now apply it to describe the normal state transport properties of Tl2201 from optimum doping through to the heavily overdoped side. I chose Tl2201 as the model system for several important reasons; (i) Tl2201 is a single band cuprate, and therefore does not contain any secondary conducting subsystem, such as CuO chains, that

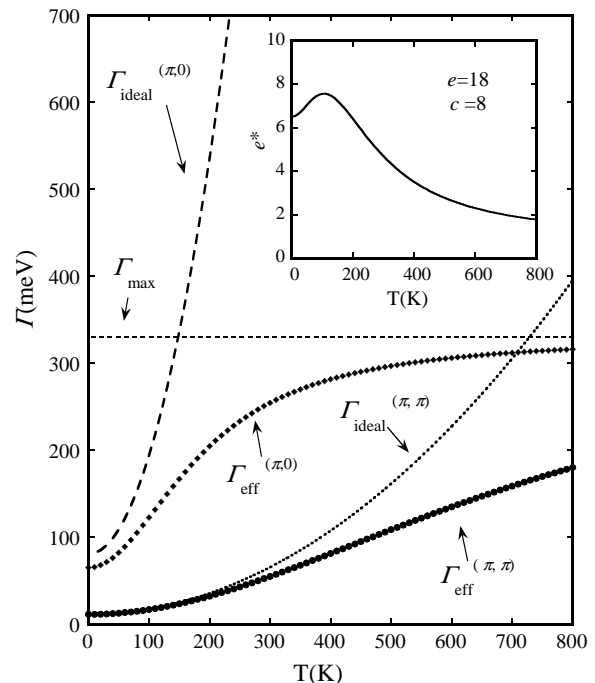


FIG. 1. T -dependence of the ideal and effective scattering rates for $(\pi, 0)$ and (π, π) within the model. Dashed line; $\Gamma_{\text{ideal}}(T)$ for $(\pi, 0)$; dotted line; $\Gamma_{\text{ideal}}(T)$ for (π, π) ; closed diamonds; $\Gamma_{\text{eff}}(T)$ for $(\pi, 0)$; closed circles; $\Gamma_{\text{eff}}(T)$ for (π, π) . The parameters for each one are given in the text. Inset: T -dependence of the effective anisotropy $e^* = \Gamma_{\text{eff}}^{(\pi,0)}/\Gamma_{\text{eff}}^{(\pi,\pi)}$.

might complicate Hall conductivity or magnetoresistance data; (ii) it has a single CuO_2 plane and therefore is not complicated by bilayer coupling; (iii) the doping range of Tl2201 single crystals covers only the OD region of the phase diagram and therefore avoids any additional complications due to the normal state pseudogap; (iv) it shows the most striking separation of the transport and Hall lifetimes (at optimum doping);²⁴ and (v) a T -dependent anisotropy in the in-plane scattering rate has already been observed in OD Tl2201 ($T_c = 30\text{K}$), as described above.¹⁸

In the Boltzmann transport equation, both the Fermi wave vector k_F and the Fermi velocity v_F are required, and to be consistent with band structure calculations,²⁵ I introduce a small degree of anisotropy in both $k_F(\phi)$ ($= k_{F0}(1 + \alpha \sin^2 2\phi)$; $\alpha = 0.15$) and $v_F(\phi)$ ($= v_{F0}(1 + \beta \sin^2 2\phi)$; $\beta = 0.20$). These small anisotropy factors do not play a significant role in the following analysis and for simplicity, are assumed to be independent of doping concentration. I take $k_{F0} = 0.65 \text{ \AA}^{-1}$, consistent with a doping level $p = 0.16$ (for $\alpha = 0.15$), and $v_{F0} = 2 \times 10^5 \text{ ms}^{-1}$. This leads to a corresponding saturation scattering rate $\Gamma_{\max} = 500 \text{ THz}$ or 340 meV (since $a = 3.86 \text{ \AA}$). Again, these values are kept constant for all doping concentrations studied here. Thus in the ensuing analysis,

there are only two adjustable parameters, namely the two anisotropy parameters c and e .

Fig. 2 shows $\rho_{ab}(T)$ and $\cot\Theta_H(T)$ data for OP Tl2201 ($T_c = 80\text{K}$) taken on the same single crystal²⁴ (the experimental data are represented by closed circles). $\rho_{ab}(T)$ and $\cot\Theta_H(T)$ show the very simple linear and quadratic T -dependencies characteristic of OP cuprates. This clean separation of the transport and Hall lifetimes is one of the central hallmarks of cuprate physics and has been one of the strongest challenges for any transport model to address. One surprising feature of the experimental data shown in Fig. 2, is that the zero-temperature intercept for $\rho_{ab}(T)$ (extrapolation indicated by a dotted line) is small and *negative*, whilst for $\cot\Theta_H(T)$, it is large and *positive*. Straight line fits to the experimental data between 130K and 300K give $\rho_{ab}(T) = -10 + 1.56T$ ($\mu\Omega\text{cm}$) and $\cot\Theta_H(T) = 270 + 0.014T^2$ (in 1 Tesla).²⁴

As argued in section II, the T -dependence of $\cot\Theta_H(T)$ is taken to represent the intrinsic T -dependence of $\Gamma_{\text{ideal}}^{(\pi,\pi)}(T)$. Given k_{F0} and v_{F0} , we obtain $A = 18$ THz and $B = 0.00093$ THz/K². Together with $\Gamma_{\text{max}} = 500$ THz, this completely defines $\Gamma_{\text{eff}}(\phi, T)$ for insertion into the Boltzmann expressions for $\rho_{ab}(T)$, $\cot\Theta_H(T)$ and $\Delta\rho_{ab}/\rho_{ab}(T)$. I reiterate here that apart from numerical factors governed by our choice of k_{F0} and v_{F0} , there are no adjustable parameters in the fitting routine other than c and e .

The best fits to $\rho_{ab}(T)$ and $\cot\Theta_H(T)$ are shown as solid lines in Fig. 2 for $c = 8$ and $e = 18$.²⁶ In the temperature interval between 130K and 300K, both a linear resistivity and a quadratic Hall angle are obtained from a single T^2 quasi-particle scattering rate. Moreover, between 130K and 300K, both the slopes and the (extrapolated) $T = 0$ intercepts are found to be in excellent agreement with the experimental data. Below 130K, the fit to $\rho_{ab}(T)$ deviates from linearity, approaching T^2 as T goes to zero. The experimentally determined $\rho_{ab}(T)$ actually shows a downward deviation from linearity below 130K, indicating the onset of superconducting fluctuations which always dominate the intrinsic normal state $\rho_{ab}(T)$ near T_c . As expected, the T dependence of $\cot\Theta_H(T)$ is almost identical to that of $\Gamma_{\text{ideal}}(T)$ in good agreement with Ong's picture.¹⁹

The insets in Fig. 2 show fits to $\rho_{ab}(T)$ and $\cot\Theta_H(T)$ over an extended temperature range up to 500K and reveal the influence of Γ_{max} and the onset of saturation above 360K. The fact that this tendency towards saturation is not actually observed in HTC is puzzling and undoubtedly raises the question whether this model is really appropriate for the HTC problem. However, as I argue in section IV, there are several possible factors that might lead to a non-saturating resistivity in HTC which go beyond conventional Boltzmann transport analysis and mask the intrinsic behavior of the scattering rate at higher temperatures.

An equally strong challenge to the more conventional models of HTC transport has been the T -dependence and magnitude of $\Delta\rho_{ab}/\rho_{ab}(T)$ and in particular the observa-

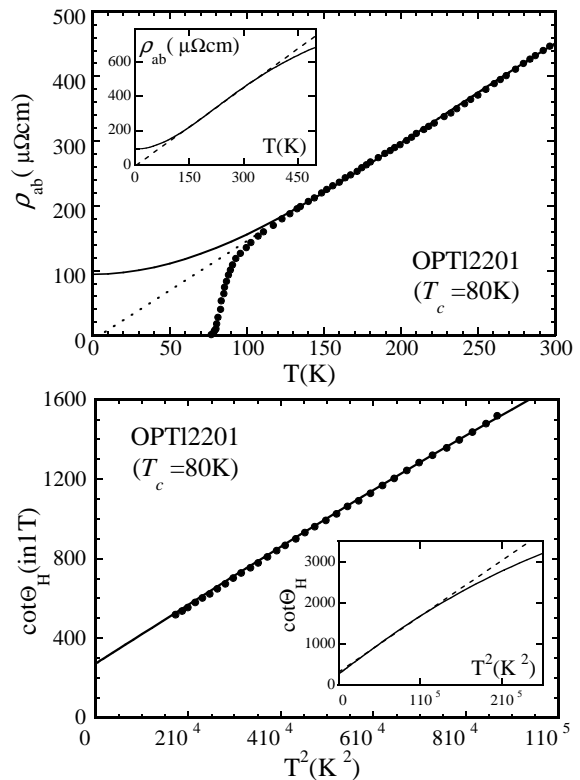


FIG. 2. Top: $\rho_{ab}(T)$ data (closed circles) for OP Tl2201.²⁴ The solid line is a fit to the data for $c = 8$ and $e = 18$. Note the upward deviation of $\rho_{ab}(T)$ below 130K. The dotted line is a guide to the eye. Bottom: $\cot\Theta_H(T)$ data (closed circles) for the same crystal.²⁴ The solid line is the fit with the same parameters. Insets: The same fits up to 500K, showing the onset of saturation at higher T .

tion of a modified Kohler's rule $\Delta\rho_{ab}/\rho_{ab} = m^2 \tan^2\Theta_H$.³ Fig. 3 shows $m(T)$ (open circles) for OP Tl2201 calculated using the same model parameters that were used in Fig. 2. Between 0K and 300K, m changes by approximately 20% with an average value of 2.6. Above 100K, the change is even smaller ($\pm 5\%$).²⁷ Experimentally, m has an approximately constant value (in the low-field limit) of 1.9 down to 130K, as indicated in the figure by a horizontal dashed line.²⁸ Below this temperature, superconducting fluctuations again begin to dominate. Also shown in the figure (as dotted lines) are the experimentally determined values of m for OP LSCO³ and OP YBCO.³ As one can see, the calculated m lies close to the measured value for OP Tl2201 and well within the experimental range for OP cuprates. It should be noted here that increasing the Fermi surface anisotropy (α) brings m even closer to the real value. It should also be noted that the present model does not include vertex corrections²⁹ nor paraconductivity contributions that might influence the form of $\Delta\rho_{ab}/\rho_{ab}(T)$, particularly at low T .

Finally for OP Tl2201, I mention here briefly the possible effect of impurities on $\rho_{ab}(T)$ and $\cot\Theta_H(T)$ within

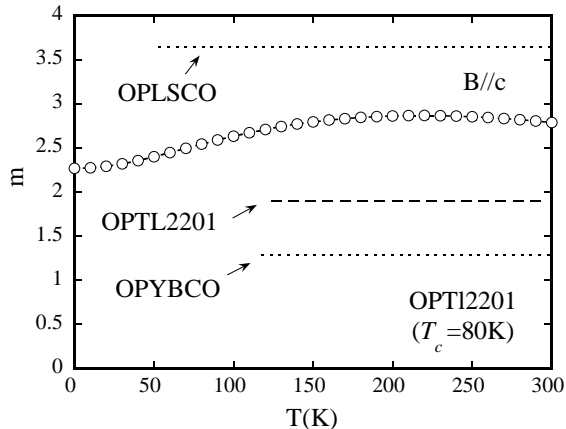


FIG. 3. Modified Kohler's plot for OP Tl2201. The open circles show the T -dependence of m (where $m^2 = (\Delta\rho_{ab}/\rho_{ab})/(\tan^2\Theta_H)$) obtained with the same fitting parameters as used in Fig. 2). The dashed line indicates the value of m determined experimentally for OP Tl2201,²⁸ while the dotted lines represent the experimental values for OP LSCO³ and OP YBCO.³

the present approach. To simulate the addition of impurities (e.g. Zn substitution in the CuO_2 plane), one would simply increase the isotropic term in $\Gamma_0(\phi)$ whilst keeping all other parameters constant. Unfortunately, such an experimental study has not yet been carried out for OP Tl2201. However, given the form of $\Gamma_{\text{ideal}}(\phi, T)$, it is easy to see that Matthiessen's rule will hold, at least for low levels of impurity, since the scattering rates are additive. At higher impurity levels however, the influence of Γ_{max} on $\Gamma_{\text{eff}}(\phi, T)$ will become manifest and deviations from Matthiessen's rule are expected.

At this stage, it is perhaps worth comparing the present model with the "Cold Spots" model of Ioffe and Millis,⁷ that has conceptually similar phenomenology and has had relative success in explaining some of normal state transport properties in OP HTC. In their model, the effective scattering rate contains two terms added in series, an isotropic FL scattering rate $1/\tau_{FL} \sim T^2$ and a T -independent scattering rate $\Gamma_0(\phi)$ that is large everywhere except the nodal directions (In some sense this plays the role of Γ_{max}). From this phenomenological picture, apparent separation of the transport and Hall lifetimes is achieved, but the parameters required to separate the two yield an orbital magnetoresistance that is extremely large and has a much stronger T -dependence than shown in Fig. 3.⁷ In addition, Matthiessen's rule is strongly violated since the Cold Spots model predicts a residual resistivity ρ_0 scaling as $(\Gamma_0/\tau_{FL})^{1/2}$. It appears that both these failings are overcome by the present model. Firstly, the introduction of the "shunt" Γ_{max} makes the effective anisotropy around the Fermi surface much smaller (see inset to Fig. 1), thereby reducing both the magnetoresistance and the T -dependence of $\Delta\rho_{ab}/\rho_{ab}(T)$. Secondly, in contrast to the Cold Spots

model, the elastic and inelastic scattering rates here are additive and deviations from Matthiessen's rule are only expected at high T and for high impurity levels when the momentum-averaged $\Gamma_{\text{ideal}}(T)$ becomes comparable to Γ_{max} .

To complete the analysis of the normal state transport properties in Tl2201, I consider here their evolution with doping. The top panel in Fig. 4 shows experimental $\rho_{ab}(T)$ data for two OD Tl2201 single crystals with T_c values of 55K and 30K.²⁸ Again the closed circles are the raw data and the solid lines the best fits to $\Gamma_{\text{eff}}(\phi, T)$. The fitting parameters are $c = 3$, $e = 9$ for the 55K crystal, and $c = 3$, $e = 5$ for the 30K crystal. The coefficients A and B are taken from the experimental data²⁸ whilst k_{F0} , v_{F0} and Γ_{max} are unchanged. Note that the anisotropy factors are markedly reduced when compared to OP Tl2201. The bottom panel in Fig. 4 shows $\cot\Theta_H(T)$ for the two samples. In contrast to OP Tl2201, the simulated $\cot\Theta_H(T)$ curves deviate slightly from a simple T^2 dependence. In fact, the T -dependence for both samples is closer to $T^{1.9}$ than T^2 . This deviation from a T^2 dependence probably reflects the fact that in the less anisotropic OD cuprates, other regions of the Fermi surface are beginning to contribute to the Hall angle.³⁰ The inset in the bottom panel in Fig. 4 gives the modified Kohler's plot derived for the two doping levels. As we expect, m is lower in these examples compared with OP Tl2201, with values approaching 2.0 and 1.6 for the 55K and 30K crystal respectively. Experimentally, m is found to be 1.4 for 30K Tl2201 (as indicated by the dashed line),²⁸ again in excellent agreement with the model.

IV. DISCUSSION

The excellence of the fits described above ought by itself to be reasonable justification for the assumptions proposed in this model. However, the current proposal appears, at first sight at least, to be incompatible with two key aspects of the experimental situation; namely the linear resistivity at low T and the absence of resistivity saturation at high T . Therefore, before going on to discuss the possible implications of the model, it is perhaps worth outlining to the reader how these two major discrepancies might possibly be reconciled.

It has often been claimed that the linear $\rho_{ab}(T)$ observed in OP HTC is the intrinsic T -dependence for all $T > 0$. This long-held view is based largely on the observation back in 1990 of a linear $\rho_{ab}(T)$ in single crystal $\text{Bi}_2\text{Sr}_2\text{CuO}_{6+\delta}$ (Bi2201) extending from $T_c = 10\text{K}$ up to 700K.³¹ If this were indeed the intrinsic behavior, it would certainly require an explanation outside the realms of conventional FL physics. Important new data on the latest generation of Bi2201 single crystals (with significantly improved T_c values) tell a rather different story. By suppressing superconductivity in OP Bi2201 ($T_c =$

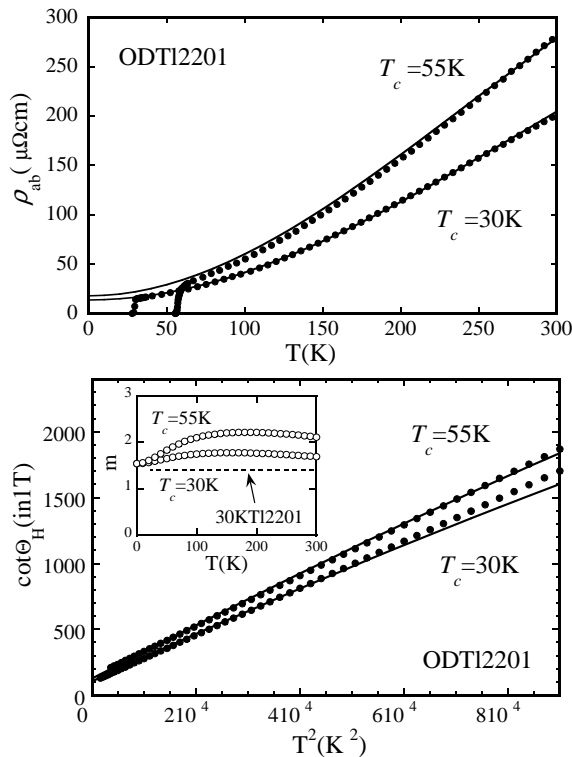


FIG. 4. Top: $\rho_{ab}(T)$ data²⁸ (closed circles) and model fits (solid lines) for OD TI2201 ($T_c = 55\text{K}$ and $T_c = 30\text{K}$). Bottom: $\cot\Theta_H(T)$ data²⁸ (closed circles) and model fits (solid lines) for the same samples with the same fitting parameters. Inset: Modified Kohler's plot (open circles) for the two doping levels within the same model. Experimental data²⁸ for the 30K crystal are indicated by a dashed line.

32K) in a 60 Tesla pulsed magnetic field, Ono *et al.*³² recently found that the linear $\rho_{ab}(T)$ seen at high T (and giving an apparent zero intercept at $T = 0\text{K}$) crosses over to a higher power T -dependence below around 60K, before saturating at some finite *positive* ρ_0 . Similar behavior has also been reported by the same group in OP $\text{La}_{2-x}\text{Sr}_x\text{CuO}_4$ ($x = 0.17$) again under high magnetic fields.³³

Another important, but often overlooked feature of transport data in HTC is the (extrapolated) negative intercept in $\rho_{ab}(T)$ seen in the best quality samples.^{24,34} Such a negative intercept is of course physically unfeasible. $\rho_{ab}(T)$ must cross over to a higher power of T at lower temperatures. Such behavior is incompatible with the MFL hypothesis, for example, but is a natural consequence of the form of $\Gamma_{\text{eff}}(\phi, T)$ presented here. Clearly, this long-standing assertion that $\rho_{ab}(T)$ obeys a simple linear T -dependence at low T should now be re-examined. It would certainly be interesting to follow the T -dependence of OP cuprates with higher T_c to lower temperatures, as and when larger magnetic fields become available.

I now turn to address the second point, the absence of

resistivity saturation at higher temperatures. The MIR limit has been a cornerstone of metallic physics for many years and the parallel-resistor model has been applied successfully to a wide range of materials. Its relevance to strongly correlated electron systems such as HTC, however, has been challenged in recent times.³⁵ In these so-called "bad metals", $\rho(T)$ does not saturate. Instead $\rho(T)$ grows approximately linearly with T at high temperatures (typically $T > 300\text{K}$) reaching values of the order 1 - 10 $\text{m}\Omega\text{cm}$ that correspond to $\ell \ll a$. It is claimed that this absence of resistivity saturation is a signature of a non-FL ground state at zero temperature.³⁵ At first sight, these arguments appear rather compelling. However, the origin of the non-saturating resistivity in these systems is still poorly understood. More importantly, similar $\rho(T)$ behavior has also been reported in Sr_2RuO_4 ,³⁶ a close structural analog of the cuprates which exhibits quantum oscillations³⁷ and so forms a well-defined FL ground state at low T . The association of non-saturating $\rho(T)$ with a non-FL ground state is therefore misleading and dictates that some other physical origin be sought for the high- T behavior.

Possible sources for the excess resistivity include thermal expansion effects (known to play a significant role in organic conductors, for example), thermally-induced reduction in the density of states or carrier concentration, and the onset of a "thermal" diffusive (non-Boltzmann) transport regime at high T once the concept of a scattering rate is no longer applicable and temperature becomes the only relevant energy scale in the problem. Determining the origin of this non-saturating resistivity, though desirable, is not essential for justifying the model however, since the model is only strictly applicable in the low- T ($T < 300\text{K}$) regime, where the majority of the carriers are still well-defined quasi-particles and Boltzmann transport analysis remains valid.

Of course, in order for the model to be applicable to HTC, it is necessary to find evidence for saturation in $\Gamma_{\text{eff}}(\phi, T)$ (or more formally ℓ), and to do this, one should appeal to experiments in which the quasi-particle scattering rate can be determined separately from the resistivity. ARPES provides one means of achieving this, since the width of the single-particle spectral function gives a direct measure of the imaginary part of the self-energy or single-particle scattering rate $\text{Im}\Sigma$. In the most naive picture, $\text{Im}\Sigma = \Gamma/2$. Given $\Gamma_{\text{max}} = 150 - 450$ meV for HTC, the corresponding maximum for the self energy $\text{Im}\Sigma_{\text{max}}$ is estimated to lie between 75 and 225 meV.

Intriguingly, the ARPES community have already shown evidence suggestive of such a threshold. Under reasonable assumptions, the Argonne group recently extracted $\text{Im}\Sigma$ from their own ARPES spectra along $(\pi, 0)$ for slightly OD $\text{Bi}_2\text{Sr}_2\text{CaCu}_2\text{O}_8$ ($\text{Bi}2212$)¹⁴ and found that it saturated above T_c at a value $\text{Im}\Sigma_{\text{max}} \sim 90$ meV inside our range of validity for $\ell = a$. More recently still, Valla *et al.*³⁸ reported strong lifetime anisotropy within the basal plane of OP $\text{Bi}2212$ and at $(\pi, 0)$, where the scattering was strongest, they also observed a tendency

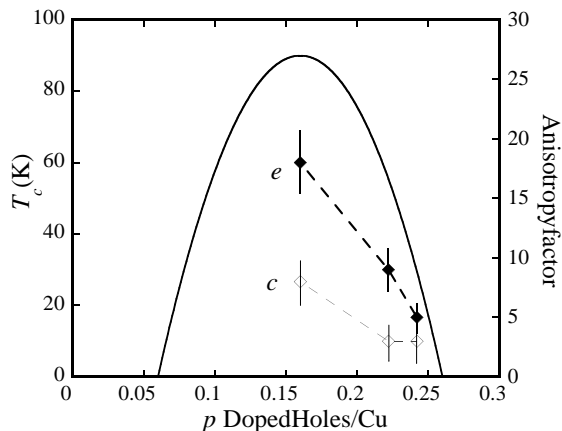


FIG. 5. Variation of the anisotropy factors c (open diamonds) and e (closed diamonds) with doping concentration p . The dashed lines are guides to the eye. The solid line represents the $T_c(p)$ parabola for HTC.⁴⁰

towards saturation above T_c at a value corresponding to $\ell = 6\text{\AA} \sim a$. All these observations are consistent with the present model and reinforce the argument that saturation in $\text{Im}\Sigma$ or Γ may occur in HTC. Whether this picture is applicable to the other correlated electron systems remains to be seen, though recent analysis of plasmon spectra in K_3C_{60} ,³⁹ another system with non-saturating resistivity, has revealed a quasi-particle scattering rate that also saturates around $T = 500\text{K}$ at a value $\Gamma_{\text{max}} \sim 450\text{ meV}$. It is still conceivable therefore that the MIR limit is a preserve of *all* metallic systems, in the strictest sense that the quasi-particle scattering rate never exceeds the maximum value Γ_{max} corresponding to $\ell = a$, and that the excess resistivity seen in these strongly correlated systems should in no way be regarded as a signature of an ever increasing scattering rate.

The most striking features of the analysis described in Section III are the large values for the anisotropy factors c and e extracted from the fitting routine and their strong variation with doping. This is summarized in Fig. 5 where we plot c (open diamonds) and e (closed diamonds) versus doping concentration p . For each crystal, p is obtained from the well-known HTC parabola law $T_c(p)/T_c^{\text{max}} = 1 - 82(p - 0.16)^2$,⁴⁰ shown as a solid line in Fig. 5. The error bars reflect the range of fitting parameters that provide a reasonable fit to all the transport properties considered here.

The large value of c , particularly at optimum doping, is somewhat surprising, though a similar degree of anisotropy in the elastic part of the single-particle self-energy has recently been inferred from ARPES measurements in $\text{Bi}2212$.³⁸ It has been suggested too that scattering on impurities located *off* the CuO_2 planes favours forward scattering (small momentum transfer) and leads naturally to a four-fold anisotropy in $\Gamma_0(\phi)$.¹⁰ In the case of tetragonal $\text{Tl}2201$, such interplane randomness might

be induced by Tl/Cu site substitutions as well as by interstitial oxygen. It is not clear at this stage why such large anisotropy would also appear in the zero-field transport scattering rate, which typically depends only on large-momentum transfers. However, as noted by Varma *et al.*,¹⁰ this anisotropic elastic term may well play a key role in the *magneto*-transport behaviour. As it happens, the main reason for having such a large value for c in our fitting routine is to maintain the constancy of $m(T)$ (i.e. the ratio of the magnetoresistance and the square of the Hall angle) down to low temperatures.

The more significant anisotropy factor e is found to drop steeply from optimum doping, almost scaling with T_c and approaching zero (corresponding to an isotropic scattering rate) close to the doping level where superconductivity vanishes. This is to be expected, perhaps, since the separation of transport and Hall lifetimes is observed to vanish in the most highly OD samples.⁴¹ The large value for e at optimum doping implies the existence of a singular scattering mechanism, peaked at $(\pi, 0)$, whose intensity grows rapidly with decreasing carrier concentration. The correlation between $e(p)$ and $T_c(p)$ on the OD side is also intriguing and suggests that the mechanism giving rise to this strongly anisotropic scattering rate might also be associated with the anisotropy (*d*-wave pairing symmetry) of the superconducting order parameter in HTC. The disappearance of this catastrophic scattering mechanism below T_c is also consistent with the large increase in the quasi-particle lifetime below T_c observed in conductivity measurements.^{15,16} I do not wish to speculate at this stage on the origin of $\Gamma_{\text{eff}}(\phi, T)$, though one possible candidate, particularly given the form of the anisotropy and its singular nature, is the collective magnetic resonance mode seen in neutron scattering measurements on several cuprates including $\text{Tl}2201$.⁴² It is noted with caution, however, that this mode has so far only been unambiguously resolved below T_c , so its relevance to scattering in the normal state has yet to be established.

As illustrated in Fig. 1, $\Gamma_{\text{ideal}}(\pi, 0)$ for OP $\text{Tl}2201$ is found to cross the MIR limit close to $T = T_c$. (The effective scattering rate at this point will obviously be lower than the saturation value, due to the presence of the shunt Γ_{max} .) The picture that emerges then is one in which the quasi-particles at the anti-nodal sites are approaching an incoherent state at $T = T_c$, consistent with what is observed in ARPES,²³ and this may well have implications for the onset temperature of superconductivity on the underdoped (UD) side of the phase diagram. For instance, if the anisotropy factor e continues to grow with decreasing p , the temperature at which the anti-nodal quasi-particles become incoherent will decrease accordingly. What ultimately causes the suppression of T_c on the UD side of the phase diagram is of course still open to speculation, and I cannot address that important question here, since clearly, the physics of the UD cuprates is also heavily influenced by the opening of the pseudogap which cannot be accounted for within this simple phenomenological model. Nevertheless, the onset

of incoherent quasi-particles at $T = T_c^{\text{opt}}$ is an intriguing observation from the above analysis, hints at a new interpretation of the $T_c(p)$ parabola across the HTC phase diagram and should be investigated further.

V. CONCLUSIONS

In summary, I have demonstrated for the first time how the seemingly anomalous dc transport properties of HTC may be accounted for consistently within a Boltzmann transport analysis with a single T^2 scattering rate that varies markedly around the basal plane. By invoking the MIR limit in its strictest sense, I have removed at a stroke several of the inconsistencies that plagued previous FL models based on an anisotropic scattering rate. In particular, the separation of transport and Hall lifetimes, the modified Kohler's rule, Matthiessen's rule for both $\rho_{ab}(T)$ and $\cot\Theta_H(T)$ and the evolution of the transport properties across the OD region of the phase diagram can all be reproduced with a single set of parameters. This remarkable success strongly suggests that a conventional Boltzmann transport approach might be more appropriate to describe the normal state of HTC (at least on the OD side of the phase diagram) than was previously imagined.

The form of $\Gamma_{\text{eff}}(\phi, T)$ is also consistent with several features of the single-particle spectral function identified by ARPES, including the strong basal plane anisotropy (both in the zero-temperature and the T -dependent scattering terms) and the tendency towards saturation along $(\pi, 0)$, together with the strong reduction of $\text{Im}\Sigma$ below T_c seen in conductivity measurements. It remains to be seen whether the disappearance of such a catastrophic scattering mechanism could alone provide the energy imbalance necessary to account for high temperature superconductivity.⁴³

There are still many open questions to address of course before a complete picture of the normal state can emerge. For example, it will be necessary to seek further evidence of saturation in the scattering rate, to determine the origin of $\Gamma_{\text{ideal}}(\phi, T)$ and the source of the non-saturating resistivity, and to investigate what other properties of HTC might be explicable by this model. Nevertheless, I believe these questions can be addressed and possibly hold the key to a deeper understanding of the anomalous transport properties of the cuprates.

The fact that the parent HTC compound at half-filling is an antiferromagnetic Mott insulator rather than a metal has pointed clearly to the role of strong electron correlations in the square planar CuO_2 lattice as a key element in the cuprate problem. The introduction of holes into a highly correlated 2D magnetic background is believed to give rise to a non-FL ground state at low doping, characterized by the highly anomalous physics of the UD cuprates, and ultimately, unconventional high temperature superconductivity. It has often been assumed,

moreover, that with continued doping, HTC eventually evolve into a conventional FL as the electron correlations become weaker and the system becomes more three-dimensional. In this paper, I have identified a form for the normal state scattering rate that although somewhat unconventional, is still rooted in FL physics, yet can explain the evolution of the normal state transport properties of OD HTC right up to optimum doping. Of course, I do not expect this simple model to remain valid on the UD side of the phase diagram, but if this proposal for the quasi-particle scattering rate is proven to hold for OD and OP cuprates, then the way in which this relatively simple picture breaks down, as the pseudogap opens and electron correlations become even stronger, might yet reveal the crucial missing link between the FL fixed point on the overdoped side and the curious physics of HTC on the underdoped side.

VI. ACKNOWLEDGEMENTS

The author would like to acknowledge enlightening discussions with J.F. Annett, K. Behnia, A. Carrington, J.R. Cooper, I.R. Fisher, B.L. Gyorffy, J.W. Loram, A.P. Mackenzie, N. Nagaosa, K.G. Sandemann, A.J. Schofield, H. Takagi, J.L. Tallon and J.A. Wilson. The author also would like to acknowledge the hospitality of the University of Tokyo where many of these ideas were first formulated.

VII. APPENDIX: TRANSPORT COEFFICIENTS FOR A QUASI-2D FERMI SURFACE

The current response \mathbf{J}_i to an applied electric \mathbf{E} is given by

$$\mathbf{J}_i = \frac{1}{4\pi^3} \int e v_i g_k d^3k = \sigma_{ij} \mathbf{E}_j$$

where g_k is the displacement from the equilibrium distribution ($g_k = f - f_0$) due to the applied fields, σ_{ij} is the conductivity tensor and v_i is the Fermi velocity in the i direction. The total displacement can be summarized in the Bloch-Boltzmann transport equation, which under the relaxation time approximation, is given by

$$e\mathbf{E} \cdot \mathbf{v}_k \frac{\partial f_0}{\partial \varepsilon} + \frac{e}{\hbar} [\mathbf{v}_k \times \mathbf{B}] \frac{\partial g_k}{\partial k} = -g_k \Gamma$$

The various components of $\sigma_{ij}^{(n)}$ can be obtained through the Jones-Zener expansion

$$g_k^{(n)} = \left(-\frac{e}{\hbar\Gamma} [\mathbf{v}_k \times \mathbf{B}] \frac{\partial}{\partial k} \right)^n \left(\frac{e\mathbf{E} \cdot \mathbf{v}_k}{\Gamma} \left(-\frac{\partial f_0}{\partial \varepsilon} \right) \right)$$

to arrive at:

$$\sigma_{ij}^{(n)} = \frac{1}{4\pi^3} \int e v_i \left(-\frac{e}{\hbar\Gamma} [\mathbf{v}_k \times \mathbf{B}] \frac{\partial}{\partial k} \right)^n \frac{e v_j}{\Gamma} \left(-\frac{\partial f_0}{\partial \varepsilon} \right) d^3k$$

To calculate, for instance, the in-plane Hall conductivity $\sigma_{xy}^{(1)}$, we simply apply B_z and E_y and calculate the response J_x using the Jones-Zener term $g_k^{(1)}$.

For a quasi-2D Fermi surface, there are various techniques one can adopt to simplify the calculation. Firstly, the element d^3k is the product of an area parallel to the Fermi surface dS and a radial (in-plane) component dk_r which is related to an incremental energy $d\varepsilon$ by

$$d\varepsilon = \hbar v_F k_F = \hbar v_F \cos \gamma dk_r$$

Here γ is the angle between v_F and dk_r (within the plane). Since v_F is always perpendicular to the Fermi surface, simple geometrical considerations give

$$\gamma(\phi) = \tan^{-1} \left[\frac{\partial}{\partial \phi} (\log k_F(\phi)) \right]$$

which is zero for a circular Fermi surface.

The element dS can be expanded into the cylindrical elements $k_F d\phi$ and dk_z to give

$$\int (-\frac{\partial f_0}{\partial \varepsilon}) d^3k = \int_0^{2\pi} \int_{-\pi/d}^{\pi/d} \frac{k_F}{\hbar v_F \cos \gamma}$$

for a quasi-2D Fermi liquid since $(-\partial f_0/\partial \varepsilon)$ is a delta function (provided all scattering is quasi-elastic). It is this integral $\int d\phi$ that will contain all the in-plane anisotropy of the essential parameters in our calculation. With $B \parallel c$, the cross-product $[\mathbf{v}_k \times \mathbf{B}] \partial/\partial k$ becomes $B v_F \partial/\partial k_{\parallel}$ where

$$\frac{\partial}{\partial k_{\parallel}} = \frac{\cos \gamma}{k_F} \frac{\partial}{\partial \phi}$$

whilst for $B \parallel ab$, making an angle φ with the a -axis

$$[\mathbf{v}_k \times \mathbf{B}] \frac{\partial}{\partial k} = v_z [\hat{\mathbf{z}} \times \mathbf{B}] \frac{\partial}{\partial k_{xy}} + [\mathbf{v}_{xy} \times \mathbf{B}] \frac{\partial}{\partial k_z}$$

i.e.

$$[\mathbf{v}_k \times \mathbf{B}] \frac{\partial}{\partial k} \approx B v_F \sin(\phi - \gamma - \varphi) \frac{\partial}{\partial k_z}$$

Finally, it is noted that the tetragonal symmetry of Tl2201 allows the limits of integration to be reduced to 0 and $\pi/2$ by including an extra factor of 4.

Employing these simple techniques, we can now derive the individual terms of the in-plane and c -axis conductivity tensor. In this paper, we are only interested in the in-plane magneto-transport properties and below we list their formulae, in the isotropic case. For the anisotropic case, simply replace v_F , k_F and Γ by $v_F(\phi)$, $k_F(\phi)$ and $\Gamma(\phi)$, or in the present case, $\Gamma_{\text{eff}}(\phi, T)$.

$$\sigma_{xx}^{(0)} = \frac{e^2}{4\pi^3 \hbar} \left(\frac{2\pi}{d} \right)^4 \int_0^{\pi/2} \frac{k_F v_F \cos^2(\phi - \gamma)}{\Gamma \cos \gamma} d\phi$$

$$\sigma_{xy}^{(1)} = \frac{e^3 B}{4\pi^3 \hbar^2} \left(\frac{2\pi}{d} \right)^4 \int_0^{\pi/2} \frac{v_F}{\Gamma} \cos(\phi - \gamma) \frac{\partial}{\partial \phi} \left(\frac{v_F}{\Gamma} \sin(\phi - \gamma) \right) d\phi$$

$$\sigma_{xx}^{(2)} = \frac{e^4 B^2}{4\pi^3 \hbar^3} \left(\frac{2\pi}{d} \right)^4 \int_0^{\pi/2} \frac{v_F}{\Gamma} \cos(\phi - \gamma)$$

$$\frac{\partial}{\partial \phi} \left\{ \frac{v_F \cos \gamma}{\Gamma k_F} \frac{\partial}{\partial \phi} \left(\frac{v_F}{\Gamma} \cos(\phi - \gamma) \right) \right\} d\phi$$

Finally, the measurable quantities ρ_{ab} , $\tan \Theta_H$ and $\Delta \rho_{ab}/\rho_{ab}$ are obtained by inversion of the conductivity tensor:

$$\rho_{ab} = \frac{1}{\sigma_{xx}^{(0)}}$$

$$\tan \Theta_H = \frac{\rho_{xy}}{R_H B} \approx \frac{\sigma_{xy}^{(1)}}{\sigma_{xx}^{(0)}}$$

$$\frac{\Delta \rho_{ab}}{\rho_{ab}} = \frac{\sigma_{xx}^{(2)}}{\sigma_{xx}^{(0)}} - \left(\frac{\sigma_{xy}^{(1)}}{\sigma_{xx}^{(0)}} \right)^2$$

-
- ¹ M. Gurvitch and A.T. Fiory, Phys. Rev. Lett. **59**, 1337 (1987).
 - ² T.R. Chien, Z.Z. Wang and N.P. Ong, Phys. Rev. Lett. **67**, 2088 (1991).
 - ³ J.M. Harris, Y.F. Yan, P. Matl, N.P. Ong, P. W. Anderson, T. Kimura and K. Kitazawa, Phys. Rev. Lett. **75**, 1391 (1995).
 - ⁴ A. Carrington, A.P. Mackenzie, C.T. Lin, and J.R. Cooper, Phys. Rev. Lett. **69**, 2855 (1992).
 - ⁵ B.P. Stojkovic and D. Pines, Phys. Rev. Lett. **76**, 811 (1996).
 - ⁶ C. Castellani, C. di Castro and M. Grilli, Phys. Rev. Lett. **75**, 4650 (1995).
 - ⁷ L.B. Ioffe and A.J. Millis, Phys. Rev. B **58**, 11631 (1998).
 - ⁸ P.W. Anderson, Phys. Rev. Lett. **67**, 2092 (1991).
 - ⁹ C.M. Varma, P.B. Littlewood, S. Schmitt-Rink, E. Abrahams and A.E. Ruckenstein, Phys. Rev. Lett. **63**, 1996 (1989).
 - ¹⁰ C.M. Varma and E. Abrahams, Phys. Rev. Lett. **86**, 4652 (2001).
 - ¹¹ T. Valla, A.V. Fedorov, P.D. Johnson, B.O. Wells, S.L. Hulbert, Q. Li, G.D. Gu, and N. Koshizuka, Science **285**, 2110 (1999).
 - ¹² A. Lanzara, P.V. Bogdanov, X.J. Zhou, S.A. Kellar, D.L. Feng, E.D. Lu, T. Yoshida, H. Eisaki, A. Fujimori, K. Kishio, J.-I. Shimoyama, T. Noda, S. Uchida, Z. Hussain and Z.-X. Shen, Nature **412**, 510 (2001).

- ¹³ See, e.g., S.V. Borisenko, A.A. Kordyuk, S. Legner, C. Drr, M. Knupfer, M.S. Golden, J. Fink, K. Nenkov, D. Eckert, G. Yang, S. Abell, H. Berger, L. Forr, B. Liang, A. Maljuk, C.T. Lin, and B. Keimer, *Phys. Rev. B* **64**, 0904513 (2001).
- ¹⁴ M.R. Norman, M. Randeria, H. Ding and J.C. Campuzano, *Phys. Rev. B* **57**, 11093 (1998).
- ¹⁵ D.A. Bonn, Ruixing Liang, T.M. Riseman, D.J. Baar, D.C. Morgan, Kuan Zhang, P. Dosanjh, T.L. Duty, A. MacFarlane, G.D. Morris, J.H. Brewer, W.N. Hardy, C. Kallin and A. J. Berlinsky, *Phys. Rev. B* **47**, 11314 (1993).
- ¹⁶ R.C. Yu, M.B. Salamon, J.P. Lu and W.C. Lee, *Phys. Rev. Lett.* **69**, 1431 (1992).
- ¹⁷ For a good summary of anisotropic ARPES spectra in optimally doped and overdoped HTC, see Figure 3 of Z. Yosuf, B.O. Wells, T. Valla, A.V. Fedorov, P.D. Johnson, Q. Li, C. Kendziora, Sha Jian and D.G. Hinks, cond-mat/0104367.
- ¹⁸ N.E. Hussey, J.R. Cooper, J.M. Wheatley, I.R. Fisher, A. Carrington, A.P. Mackenzie, C.T. Lin, and O. Milat, *Phys. Rev. Lett.* **76**, 122 (1996).
- ¹⁹ N.P. Ong, *Phys. Rev. B* **43**, 193 (1991).
- ²⁰ Z. Fisk and G.W. Webb, *Phys. Rev. Lett.* **36**, 1084 (1976).
- ²¹ H. Wiesmann, M. Gurvitch, H. Lutz, A. Ghosh, B. Schwarz, M. Strongin, P.B. Allen and J.W. Halley, *Phys. Rev. Lett.* **38**, 782 (1977).
- ²² M. Gurvitch, *Phys. Rev. B* **24**, 7404 (1981).
- ²³ M.R. Norman, A. Kaminski, J. Mesot and J.C. Campuzano, *Phys. Rev. B* **63**, 140508(R) (2001).
- ²⁴ A.W. Tyler and A.P. Mackenzie, *Physica* **282-287C**, 1185 (1997).
- ²⁵ D.J. Singh and W.E. Pickett, *Physica* **203C**, 193 (1992).
- ²⁶ Scaling corrections of the order 20% were applied to the fits to coincide with the experimental plots. These corrections are of the order of the experimental uncertainty and uncertainties in the absolute values of k_{F0} and/or v_{F0} and are therefore not thought to have any real significance.
- ²⁷ The value of m at low T is obviously influenced by c , the extent of the anisotropy in the impurity term, and would drop to zero in the isotropic limit.
- ²⁸ A.W. Tyler, PhD. thesis (University of Cambridge) (1997).
- ²⁹ H. Kontani, *J. Phys. Soc. Japan* **70**, 1873 (2001).
- ³⁰ It is noted here that a similar tendency for n to fall as doping increases on the overdoped side has been observed in another cuprate system, see Y. Ando and T. Murayama, *Phys. Rev. B* **60**, R6991 (1999).
- ³¹ S. Martin, A.T. Fiory, R.M. Fleming, L.F. Schneemeyer, and J.V. Waszczak, *Phys. Rev. B* **41**, 846 (1990).
- ³² S. Ono, Y. Ando, T. Murayama, F.F. Balakirev, J.B. Betts and G. S. Boebinger, *Phys. Rev. Lett.* **85**, 638 (2000).
- ³³ G.S. Boebinger, Y. Ando, A. Passner, T. Kimura, M. Okuya, J. Shimoyama, K. Kishio, K. Tamasaku, N. Ichikawa and S. Uchida, *Phys. Rev. Lett.* **77**, 5417 (1996).
- ³⁴ K. Yoshida, A.I. Rykov, S. Tajima and I. Terasaki, *Phys. Rev. B* **60**, R15035 (1999).
- ³⁵ V.J. Emery and S.A. Kivelson, *Phys. Rev. Lett.* **74**, 3253 (1995).
- ³⁶ A.W. Tyler, A.P. Mackenzie, S. NishiZaki and Y. Maeno, *Phys. Rev. B* **58**, R10107 (1998).
- ³⁷ A.P. Mackenzie, S.R. Julian, A.J. Diver, G.J. McMullan, M.P. Ray, G.G. Lonzarich, Y. Maeno, S. Nishizaki and T. Fujita, *Phys. Rev. Lett.* **76**, 3786 (1996).
- ³⁸ T. Valla, A.V. Fedorov, P.D. Johnson, Q. Li, G.D. Gu and N. Koshizuka, *Phys. Rev. Lett.* **85**, 828 (2000).
- ³⁹ A. Goldoni, L. Sangaletti, F. Parmigiani, G. Comelli and G. Paolucci, *Phys. Rev. Lett.* **87**, 076401 (2001).
- ⁴⁰ J.L. Tallon, C. Bernhard, H. Shaked, R.L. Hitterman, and J.D. Jorgensen, *Phys. Rev. B* **51**, 12911 (1995).
- ⁴¹ For very overdoped Tl2201 ($T_c = 10-15K$), $\rho_{ab}(T)$ and $\cot\Theta_H(T)$ are found to vary approximately as $A + BT + CT^2$ as $T \rightarrow 0$, rather than $A + BT^2$ (A.P. Mackenzie, S.R. Julian, D.C. Sinclair and C.T. Lin, *Phys. Rev. B* **53**, 5848 (1996)). It is not known at this time, whether this is the intrinsic low T behaviour, due to the presence of some very low energy scale, or whether $\rho_{ab}(T)$ and $\cot\Theta_H(T)$ are affected by small regions in the samples having a higher T_c .
- ⁴² H.F. He *et al.*, (unpublished).
- ⁴³ M.R. Norman, M. Randeria, B. Jank and J.C. Campuzano, *Phys. Rev. B* **61**, 14742 (2000).